IEEE Transactions on Nuclear Science, Vol.NS-22, No.3, June 1975

BEAM LOADING EFFECTS IN THE CERN PS BOOSTER

F. Pedersen
MPS Division, CERN, Geneva, Switzerland

Summary and Introduction

At intensities > 1.5×10^{12} protons per ring, and at reduced RF voltage, fast growing beam loading instabilities occur in the Booster (PSB) with loss of beam bunching. The observed thresholds are reported; they are different from those given by Robinson's[1] criterion and occur with a different frequency. To explain this and other observations, a model of the beam loading interaction including the feedback loops controlling RF amplitude, phase and cavity tuning, is presented. In the general case, beam loading causes cross-coupling between all three loops, which for high beam loading makes the system unstable.

For low beam loading, which was assumed for the basic systems design, the loops are practically independent. The Robinson criterion is a limiting case of this model (no feedback loops). A method for designing better loops taking into account the cross-coupling is described. It has the advantage over other cures, such as lowering of the cavity Q or feeding the cavity with a current equal to the beam current but of opposite phase, that it does not require extra RF power.

The RF Feedback Loops in the PSB[2,3]

A simplified block diagram of the RF and beam control system is shown in Fig. 1. There are 3 important loops. The tuning loop keeps the tube current (grid voltage) in phase with the gap voltage by acting on the DC bias of the ferrite rings. This automatically ensures minimum tube current for varying frequency and beam loading. The AVC loop makes the gap voltage follow a prescribed voltage program by acting on the amplitude of the RF tube current. The phase loop controls the phase difference between gap phase and phase of the fundamental of the bunch signal by acting on the frequency or the phase of the RF tube current. The phase loop only corrects AC-variations of the beam-cavity phase; the absolute value (stable phase angle) is controlled by radial and synchronization loops. These last two loops have little effect on the dynamics, and will not be discussed here. They are easily added later as a correction to the phase loop.

Beam loading instabilities occur (i) during adiabatic trapping when the RF voltage is low, and (ii) later in the cycle if the RF voltage is deliberately lowered to combat longitudinal instabilities[5] (fitting bucket size to bunch size). The first is cured by lowering the tube impedance[4]. The second is not easily cured in this way because the cavity impedance is lower later in the cycle, and a bigger threshold increase is required. It would imply the use of a second tube[2,4] and a programming of the tube supply voltage[6].

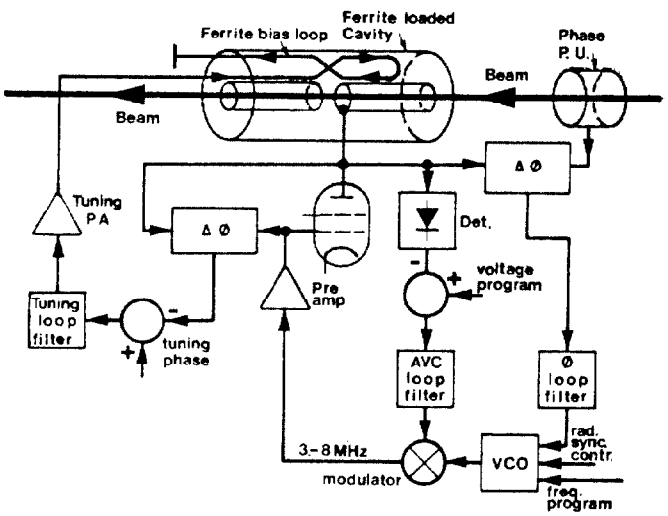

Fig. 1 : PSB RF feedback loops.

The Linearized Dynamic Model

Due to the good damping of higher order cavity modes[6], the relative low harmonic contents of generator and beam currents (long bunches), only the fundamentals of the generator and beam currents are important to determine $\bar{V}$ (Fig. 2).

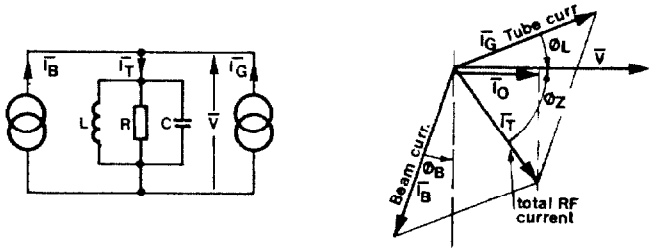

Fig. 2 : Steady state conditions.

For short bunches the amplitude of the fundamental I_B is twice the DC beam current, for the relative long PSB bunches ($\sim 180^\circ$ RF) this Fourier coefficient drops to about 1.6. The output impedance of the tube has been included in the resonant circuit equivalent so the generator can be considered as a current generator. ϕ_B is the stable phase angle ($\phi_B > 0$ = accel.), ϕ_Z is the phase angle of the cavity + tube impedance and ϕ_L is what we will call the loading phase angle. It is equal to the impedance phase angle for no beam load. I_O is the generator current required to give the same gap voltage without beam load and with the cavity tuned to resonance. The beam loading can then be characterized by a dimensionless parameter $Y = I_B/I_O$, which we will call the relative beam loading.

For a given $\bar{I}_B$ (I_B and ϕ_B) and ϕ_Z, the required I_G and ϕ_L is determined by the steady state conditions:

$$\tan\phi_L = \frac{I_O\tan\phi_Z - I_B\cos\phi_B}{I_O + I_B\sin\phi_B} = \frac{\tan\phi_Z - Y\cos\phi_B}{1 + Y\sin\phi_B} \qquad (1)$$

$$I_G = \frac{I_O + I_B\sin\phi_B}{\cos\phi_L} = \frac{I_O(1 + Y\sin\phi_B)}{\cos\phi_L} \qquad (2)$$

To determine whether a given steady state "working point" is stable or not, one has to know the transmissions from small modulations of $\bar{I}_G$, $\bar{I}_B$ (phase and amplitude) and cavity tune to $\bar{V}$. The transmissions back from modulations of $\bar{V}$ through the beam to $\bar{I}_B$ and through the "external" control electronics to $\bar{I}_G$ and cavity tune complete the loops (Fig. 3). For the beam we have assumed rigid bunches, so we get the transfer function:

$$B(s) = p_B(s)/p_V^*(s) = \omega_s^2/(s^2 + \omega_s^2) \qquad (3)$$

and no amplitude component of $\bar{I}_B$. The transfer functions for transmissions of phase and amplitude modulations through the cavity are derived in Appendix A. $C_T(s)$, $C_p(s)$ and $C_a(s)$ are the transfer functions through the control electronics. The signals on the block diagram

represent small-signal deviations from their static equilibrium values. The p's are phase deviations in radians, the a's relative amplitude deviations (e.g. $a_G = \Delta I_G/I_G$) and x is the tuning deviation relative to cavity damping rate, $x = \Delta\omega_r/\sigma$.

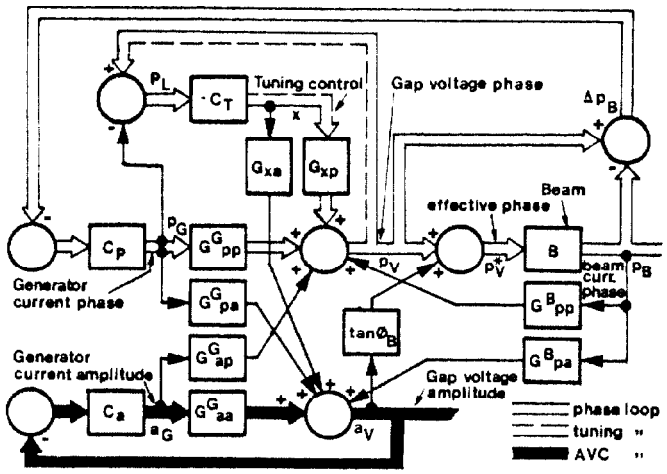

Fig. 3 : Small signal model showing transmissions between generator current, gap voltage, beam current and tuning control.

The system is unstable if the characteristic equation (B1) has roots with a positive real part. For 1st order operators in the control part of the loops (pure integration for $C_p(s)$), the equation will be of the 6th order. Although a general analytic stability analysis in principle is possible, it must be excluded due to the complexity of the coefficients. One can however get a good understanding of the dynamics of the system by considering a few limiting cases.

Although amplitude modulation of $\bar{I}_B$ has been neglected it may easily be included in the model, and the interaction between the RF system and longitudinal quadrupole type (breathing mode) oscillations[8] can be studied.

Limiting Case for No Loops

If all the loops are opened, one gets easily from the block diagram or (B1) the characteristic equation:

$$1 - B(s)(G^B_{pp}(s) + \tan\phi_B G^B_{pa}(s)) = 0 \qquad (4)$$

$$s^4 + 2\sigma s^3 + (\omega_s^2 + \sigma^2(1+\tan^2\phi_Z))s^2 + 2\sigma\omega_s^2 s$$
$$+\sigma^2\omega_s^2(1+\tan^2\phi_Z - Y\tan\phi_Z/\cos\phi_B) = 0 \qquad (5)$$

The Routh-Hurwitz criterion gives the well-known

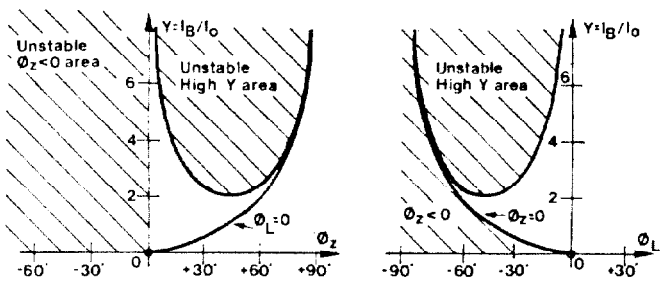

Fig. 4 : No loop stability for $\phi_B = 0$.

Robinson[1] stability condition:

$$0 < \sin 2\phi_Z < 2\cos\phi_B / Y \qquad (6)$$

which for $\phi_B = 0$ is plotted in Fig. 4. For $\phi_Z < 0$ one gets an instability with the synchrotron frequency, whilst for high Y and $\phi_Z > 0$ one gets a "zero frequency" instability with a non-oscillatory pure exponential growth.

As yet, no experiments have been performed on the Booster under these conditions where Robinson's criterion is valid.

Limiting Case for Tuning Loop Only

We simplify the problem by assuming $\phi_B = 0$, and the characteristic equation becomes:

$$1 - B(s)G^B_{pp}(s) + C_T(s)G_{xp}(s) = 0 \qquad (7)$$

A simplified loop filter $C_T(s) = \omega_T/s$, where ω_T is the bandwidth of the tuning loop, is a good approximation in a wide frequency range. Equation 7 becomes:

$$s^5 + 2\sigma s^4 + (\sigma^2(1+\tan^2\phi_Z) + \omega_s^2 + \omega_T\sigma)s^3 + (2\sigma\omega_s^2 + \sigma^2\omega_T)s^2$$
$$+(\omega_s^2\sigma^2(1+\tan^2\phi_Z - Y\tan\phi_Z) + \omega_T\sigma\omega_s^2)s + \omega_T\omega_s^2\sigma^2 = 0 \qquad (8)$$

which has stable roots if:

$$Y < \frac{(2(1+\tan^2\phi_Z) + \omega_T/\sigma)(2 - \sigma\omega_T/\omega_s^2)}{4\tan\phi_Z} \qquad (9)$$

For $\sigma\omega_T/\omega_s^2 \ll 2$ and $\omega_T/\sigma \ll 2$, (9) approaches (6), but for typical PSB parameters where $\omega_T \sim 3\omega_s$, $\sigma \sim 15\omega_s$, the (ϕ_Z,Y) diagram (Fig. 5) becomes inverted with respect to ϕ_Z.

Instabilities have been observed in the PSB in the $\phi_Z > 0$ area with Y as low as 0.15-0.20. Reduced tuning gain gives faster growth rates.

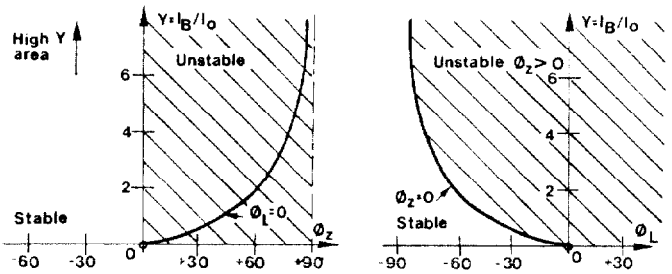

Fig. 5 : Stability with tuning loop, $\phi_B = 0$.

Limiting Case for Tuning + AVC Loops Only

As an analytical treatment is complicated, we will now use a simpler approach. In all cases without the strong feedback from the phase loop, and with a not too high beam current the system should oscillate with a frequency near to the synchrotron frequency, $s = j\omega_s + \Delta s$, and it is easy to find this shift. In Fig. 6 the total feedback from p_B to p_V^* is collected in H(s). From the characteristic equation

$$1 - B(s)H(s) = 0 \qquad (10)$$

we get

$$\Delta s = -j\omega_s H(j\omega_s)/2 \qquad (11)$$

provided $|\Delta s|$ is small compared to $2\omega_s$ or the distance to any pole or zero in H(s). A positive real part of Δs corresponds to instability.

For $\phi_B = 0$ we get for tuning + AVC loops:

$$H(s) = \frac{G^B_{pp} + C_a(G^G_{aa}G^B_{pp} - G^G_{ap}G^B_{pa})}{1 + C_aG^G_{aa} + C_TG_{xp} + C_aC_T(G^G_{aa}G_{xp} - G^G_{ap}G_{xa})} \quad (12)$$

which for our case, $|C_a(j\omega_s)| >> 1$, $\sigma >> \omega_s$ can be roughly approximated by

$$H(j\omega_s) \sim \frac{Y\tan\phi_L}{1 + \tan^2\phi_L + Y\tan\phi_L + C_T(j\omega_s)} \quad (13)$$

As $C_T(j\omega_s)$ has a negative imaginary component, we get stability for $\phi_L < 0$ and instability for $\phi_L > 0$ (Fig. 7). This agrees with observations. Also observed growth rates agree with (11) provided they are big enough for Landau damping to be neglected. Calculations show that growth rates should be higher for tuning alone than for tuning + AVC, which again agrees with observations.

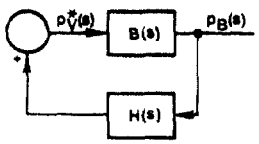

Fig. 6

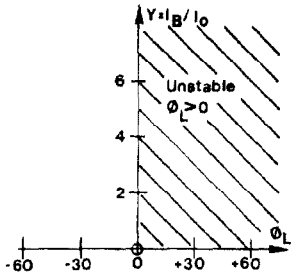

Fig. 7

The Case with AVC, Tuning and Phase Loops

This is the normal operating condition. As the phase loop produces large shifts of the synchrotron eigenvalues, the previous method cannot be used. The observations done on the 800 MeV flat top ($\phi_B = 0$) with reduced voltage (3.5 kV) showed sharp thresholds and some dependence on ϕ_L (Fig. 8). The observed frequency of instability was $\sim$ 7 kHz, while the synchrotron frequency under these conditions is $\sim$ 1 kHz. This indicates that the transmission through the beam is unimportant, so we let $B(s) = 0$. If we furthermore let $\phi_B = 0$, assume σ big, $C_a(s) = \omega_a/s$, $C_p(s) = \omega_p/s$, and $C_T(s) = \omega_T/s$, where ω_a, ω_p and ω_T are the bandwidths of the loops without beam loading, (B1) is reduced to:

$$(1+(Y+\tan\phi_L)^2)s^3 + (\omega_a+\omega_p+\omega_T+(\omega_a+\omega_p)(Y+\tan\phi_L)\tan\phi_L)s^2$$
$$+(\omega_a\omega_p+\omega_a\omega_T+\omega_T\omega_p+\omega_a\omega_p\tan^2\phi_L)s+\omega_a\omega_p\omega_T = 0 \quad (14)$$

For $\phi_L = 0$ we get the simple stability criterion:

$$Y < \sqrt{2+\frac{\omega_a}{\omega_T}+\frac{\omega_T}{\omega_a}+\frac{\omega_p}{\omega_T}+\frac{\omega_T}{\omega_p}+\frac{\omega_a}{\omega_p}+\frac{\omega_p}{\omega_a}} \quad (15)$$

which for $\omega_a = \omega_p = 5\omega_T$ gives $Y < 3.8$. From the more complicated expression including ϕ_L one can plot the thresholds (Fig. 8). These thresholds are somewhat higher than observed and the dependence on ϕ_L stronger. The frequency of instability can be worked out from (14) to be $\sim 1.5\omega_T$, which is somewhat higher than observed. From a characteristic equation including ϕ_B we get a threshold dependence of ϕ_B (Fig. 9) which agrees with observations.

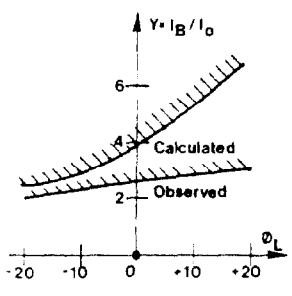

Fig. 8

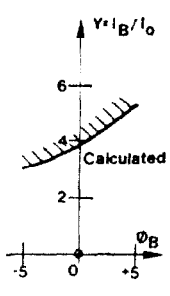

Fig. 9

Taking into account B(s) or a finite σ has a negligible effect for PSB parameters. Replacing the simple control operators assumed here with more realistic ones with lower stability phase margins has a stronger effect, especially if introduced in one of the fast loops (AVC and phase). This explains the difference in Fig. 8.

Increasing the threshold by a bigger separation of loop bandwidths (see (15)) is not very efficient (square root scaling), and can only be done to a very limited extent.

Stabilization with Decoupling Matrix

If we assume no tuning loop, $\phi_L = 0$, $\phi_B = 0$ and σ big, the object we want to control is the right part of Fig. 10. For frequencies << σ the transfer function matrix is:

$$\begin{Bmatrix} a_V(s) \\ p_V(s) \end{Bmatrix} = \frac{1}{1+Y^2(1-B(s))} \begin{Bmatrix} 1 & -Y(1-B(s)) \\ Y & 1 \end{Bmatrix} \begin{Bmatrix} a_G(s) \\ p_G(s) \end{Bmatrix} \quad (16)$$

If a decoupling matrix equal to the inverse of this matrix is inserted in front of the control object:

$$\begin{Bmatrix} a_G(s) \\ p_G(s) \end{Bmatrix} = \begin{Bmatrix} 1 & Y(1-B(s)) \\ -Y & 1 \end{Bmatrix} \begin{Bmatrix} a_C(s) \\ p_C(s) \end{Bmatrix} \quad (17)$$

as shown on the left part of Fig. 9, the transfer matrix (a_c, p_c) to (a_V, p_V) becomes a unity matrix as in the case of no beam loading.

Big DC-variations in a_c will produce big DC-variations in p_G but no change in p_V, which means that the steady state condition $\phi_L = 0$ will be violated if no tuning loop is present, or coupling to the tuning loop if this is present.

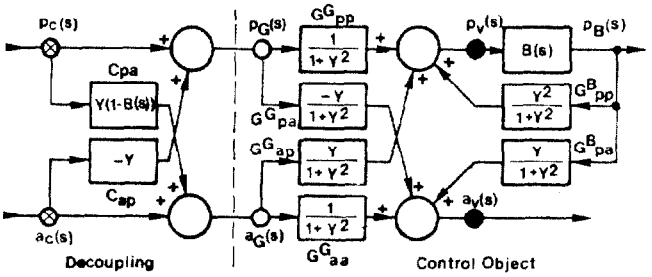

Fig. 10 : Decoupling with amplitude and phase control.

However, it is seen from Fig. 11 that since $G_{xp} = G_{pp}$ and $G_{xa} = G_{pa}$, we can just as well enter the compensation for a_c variations through the tuning x; this is in fact better as then a_c variations affect neither p_G or p_V. If x furthermore is entered through the p_c to a_G operator, the system has the same decoupled transmissions as if no beam loading was present.

It is easy to take a finite σ into account. The result is that C_{xa} and C_{xpa} must include a low pass operator $\sigma/(\sigma + s)$. The diagonal elements in the total transfer matrix will then contain the same operator, as is the case for no beam loading.

Some further manipulation of the block diagram is

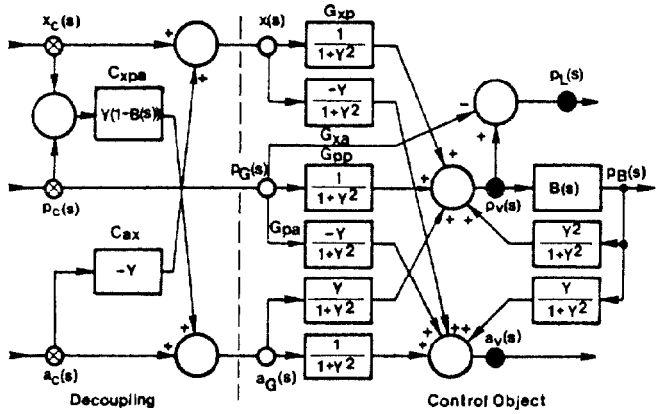

Fig. 11 : Decoupling with tuning, amplitude and phase control.

required before it can be realized. p_C is not available as a signal, since the phase modulation is done by frequency modulation (Fig. 1); however including an integration the (1 - B(s)) second order highpass operator is not a problem, and does not provide any DC-transmission. For $Y > 1$, the main transmission of the AVC is through the tuning system, which is not easily compensated for the desired bandwidth; but one can transmit the highpass part of it through p_G without affecting the tuning if this highpass part is countercompensated in p_L, and the crossover frequency is chosen properly.

Acknowledgements

I would like to thank K.H. Reich for his encouragement to carry on the work described in this paper, and F.J. Sacherer for reading the manuscript and for many helpful discussions.

References

1. K.W. Robinson, CEA, Report No. CEAL-1010 (Feb. 1964).
2. U. Bigliani et al.,IEEE Trans.Nucl.Sci.18,233 (1971).
3. U. Bigliani, IEEE Trans.Nucl.Sci. 18, 352 (1971).
4. G. Gelato et al., this conference.
5. J. Gareyte et al., this conference.
6. D. Zanaschi, private communication.
7. M. Lee, IEEE Trans.Nucl.Sci. 18, 1086 (1971).
8. H.G. Hereward, Proc. 1961 Int. Conf. Brookhaven, 236.
9. G. Nassibian, SI/Note EL/69-5.
10. U. Bigliani, SI/Note EL/69-9.

Appendix A - Phase, Amplitude and Tuning Transmissions through Cavity

If one transmits a phase- and/or amplitude-modulated sinusoidal signal:

$$i(t) = \mathrm{Re}\left\{I(1+a_i(t))\, e^{j(\omega_c t + p_i(t))}\right\}$$

through a transfer function (impedance) Z(s), the output signal will in general be both amplitude- and phase-modulated:

$$v(t) = \mathrm{Re}\left\{V(1+a_v(t))\, e^{j(\omega_c t + \phi_z + p_v(t))}\right\}$$

For low modulation indices ($a \ll 1$, $p \ll 1$), the transmissions of the modulations are linear and determined by:

$$G_{pp}(s) = G_{aa}(s) = \frac{1}{2}\left(\frac{Z(s+j\omega_c)}{Z(j\omega_c)} + \frac{Z(s-j\omega_c)}{Z(-j\omega_c)}\right) = G_S(s) \qquad (A1)$$

$$G_{pa}(s) = -G_{ap}(s) = \frac{1}{2}\left(\frac{Z(s+j\omega_c)}{Z(j\omega_c)} - \frac{Z(s-j\omega_c)}{Z(-j\omega_c)}\right) = G_C(s) \qquad (A2)$$

For a resonant circuit cavity impedance (Fig. 2) with damping rate σ, resonating at ω_r:

$$Z(s) = \frac{2\sigma R s}{s^2 + 2\sigma s + \omega_r^2} \qquad (A3)$$

and detuned an amount:

$$\omega_d = \omega_r - \omega_c = \sigma \tan\phi_z \qquad (A4)$$

from the driving frequency ω_c, we get

$$G_S(s) = \frac{\sigma^2(1+\tan^2\phi_z) + \sigma s}{s^2 + 2\sigma s + \sigma^2(1+\tan^2\phi_z)} \qquad (A5)$$

$$G_C(s) = \frac{\sigma \tan\phi_z\, s}{s^2 + 2\sigma s + \sigma^2(1+\tan^2\phi_z)} \qquad (A6)$$

These are the transmissions from modulations of $\bar{I}_T$ (Fig. 2). Taking into account, that modulations of $\bar{I}_T$ are determined by a vector sum of the modulations of $\bar{I}_B$ and $\bar{I}_G$, we get the transfer functions (Fig. 3):

$$G^G_{pp}(s) = \frac{\sigma^2(1+\tan^2\phi_z + Y(\sin\phi_B - \tan\phi_z\cos\phi_B)) + \sigma(1+Y\sin\phi_B)s}{s^2 + 2\sigma s + \sigma^2(1+\tan^2\phi_z)} \qquad (A7)$$

$$G^G_{pa}(s) = \frac{-\sigma^2 Y(\cos\phi_B + \tan\phi_z\sin\phi_B) + \sigma(\tan\phi_z - Y\cos\phi_B)s}{s^2 + 2\sigma s + \sigma^2(1+\tan^2\phi_z)} \qquad (A8)$$

$$G^G_{aa}(s) = G^G_{pp}(s);\quad G^G_{ap}(s) = -G^G_{pa}(s)$$

$$G^B_{pp}(s) = \frac{Y(\sigma^2(\tan\phi_z\cos\phi_B - \sin\phi_B) - \sigma\sin\phi_B\, s)}{s^2 + 2\sigma s + \sigma^2(1+\tan^2\phi_z)} \qquad (A9)$$

$$G^B_{pa}(s) = \frac{Y(\sigma^2(\tan\phi_z\sin\phi_B + \cos\phi_B) + \sigma\cos\phi_B\, s)}{s^2 + 2\sigma s + \sigma^2(1+\tan^2\phi_z)} \qquad (A10)$$

Tuning variations change these transfer functions, but for small variations we can neglect that and only consider the additional amplitude and phase modulations of the output caused by tuning variations. Z(s) will be a function of some tuning parameter x, Z(s,x). The transmissions from x to p_V and a_V are linear for small x:

$$G_{xp}(s) = \frac{p_V(s)}{x(s)} = \frac{\partial \arg(Z(j\omega_c,x))}{\partial x} G_S(s) - \frac{\partial |Z(j\omega_c,x)|/\partial x}{|Z(j\omega_c,0)|} G_C(s) \qquad (A11)$$

$$G_{xa}(s) = \frac{a_V(s)}{x(s)} = \frac{\partial |Z(j\omega_c,x)|/\partial x}{|Z(j\omega_c,0)|} G_S(s) + \frac{\partial \arg(Z(j\omega_c,x))}{\partial x} G_C(s) \qquad (A12)$$

If we let $x = \Delta\omega_r/\sigma$, we get from (A3), (A5) and (A6):

$$G_{xp}(s) = \frac{\sigma^2 + \sigma s}{s^2 + 2\sigma s + \sigma^2(1+\tan^2\phi_z)} \qquad (A13)$$

$$G_{xa}(s) = \frac{-\sigma^2 \tan\phi_z}{s^2 + 2\sigma s + \sigma^2(1+\tan^2\phi_z)} \qquad (A14)$$

Appendix B - Characteristic Equation for Complete System (Fig. 3)

$$\begin{aligned}
&C_a C_T (C_p(1-B)+1)(G^G_{aa}G_{xp} - G^G_{ap}G_{xa}) + C_T C_p (1-B) G_{xp} \\
&+C_a C_p (1-B)(G^G_{aa}G^G_{pp} - G^G_{ap}G^G_{pa}) + BC_a(G^G_{ap}G^B_{pa} - G^G_{aa}G^B_{pp}) \\
&+B\tan\phi_B\{C_p(G^G_{pa}G^B_{pp} - G^G_{pp}G^B_{pa} - G^G_{pa}) + C_T(G_{xa}G^B_{pp} - G_{xp}G^B_{pa}) - G^B_{pa}\} \\
&+C_p(1-B)G^G_{pp} + C_a G^G_{aa} + C_T G_{xp} - BG^B_{pp} + 1 = 0
\end{aligned} \qquad (B1)$$

where B means B(s), G_{pp} means $G_{pp}(s)$, etc.